

ISSN 007-2621

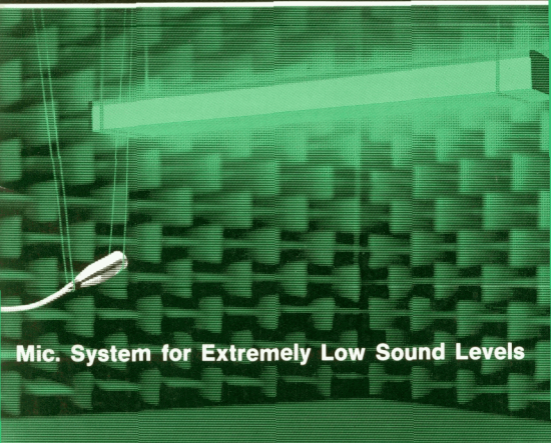
No. 3 — 1984

published quarterly

Technical Review

To Advance Techniques in Acoustical, Electrical and Mechanical Measurement

Hilbert Transform



Mic. System for Extremely Low Sound Levels

Averaging Time of Level Recorder 2317



Brüel & Kjær

**PREVIOUSLY ISSUED NUMBERS OF
BRÜEL & KJÆR TECHNICAL REVIEW**

- 2-1984 Dual Channel FFT Analysis (Part II)
- 1-1984 Dual Channel FFT Analysis (Part I)
- 4-1983 Sound Level Meters – The Atlantic Divide
Design principles for Integrating Sound Level Meters
- 3-1983 Fourier Analysis of Surface Roughness
- 2-1983 System Analysis and Time Delay Spectrometry (Part II)
- 1-1983 System Analysis and Time Delay Spectrometry (Part I)
- 4-1982 Sound Intensity (Part II Instrumentation and Applications)
Flutter Compensation of Tape Recorded Signals for Narrow Band Analysis
- 3-1982 Sound Intensity (Part I Theory).
- 2-1982 Thermal Comfort.
- 1-1982 Human Body Vibration Exposure and its Measurement.
- 4-1981 Low Frequency Calibration of Acoustical Measurement Systems.
Calibration and Standards. Vibration and Shock Measurements.
- 3-1981 Cepstrum Analysis.
- 2-1981 Acoustic Emission Source Location in Theory and in Practice.
- 1-1981 The Fundamentals of Industrial Balancing Machines and their Applications.
- 4-1980 Selection and Use of Microphones for Engine and Aircraft Noise Measurements.
- 3-1980 Power Based Measurements of Sound Insulation.
Acoustical Measurement of Auditory Tube Opening.
- 2-1980 Zoom-FFT.
- 1-1980 Luminance Contrast Measurement.
- 4-1979 Repolarized Condenser Microphones for Measurement Purposes.
Impulse Analysis using a Real-Time Digital Filter Analyzer.
- 3-1979 The Rationale of Dynamic Balancing by Vibration Measurements.
Interfacing Level Recorder Type 2306 to a Digital Computer.
- 2-1979 Acoustic Emission.
- 1-1979 The Discrete Fourier Transform and FFT Analyzers.
- 4-1978 Reverberation Process at Low Frequencies.
- 3-1978 The Enigma of Sound Power Measurements at Low Frequencies.
- 2-1978 The Application of the Narrow Band Spectrum Analyzer Type 2031 to the Analysis of Transient and Cyclic Phenomena.
Measurement of Effective Bandwidth of Filters.
- 1-1978 Digital Filters and FFT Technique in Real-time Analysis.
- 4-1977 General Accuracy of Sound Level Meter Measurements.
Low Impedance Microphone Calibrator and its Advantages.

(Continued on cover page 3)

TECHNICAL REVIEW

No. 3 — 1984

Contents

The Hilbert Transform	
N. Thrane.....	3
Microphone System for Extremely Low Sound Levels	
E. Frederiksen	16
Improved RMS Averaging with true exponential Response using the B & K Level Recorder Type 2317	
L. Thomsen	23
News from the Factory.....	31

THE HILBERT TRANSFORM

by

N. Thrane, (Ph.D.)

ABSTRACT

The theoretical background of the Hilbert Transform incorporated in the B&K Dual Channel Signal Analyzers Types 2032/2034, is introduced in this article. Using this transform, the normal real valued time domain functions are made complex, which yield two new useful properties – the Envelope and the Instantaneous Frequency. Practical use of the Envelope function is demonstrated.

SOMMAIRE

La théorie de la transformée de Hilbert incorporée dans les Analyseurs de signaux bicanaux Types 2032/2034 est présentée dans cet article. Par cette transformation, des fonctions normales en valeur réelle du domaine temporel deviennent complexes et donnent deux nouvelles propriétés très utiles: l'enveloppe et la fréquence instantanée. L'utilisation pratique de la fonction enveloppe est démontrée dans cet article.

ZUSAMMENFASSUNG

Dieser Artikel stellt den theoretischen Hintergrund der Hilbert-Transformation, die in die Brüel&Kjær Zweikanal-Signalanalysatoren 2032 und 2034 eingebaut ist, vor. Mit dieser Transformation wird aus der normalen, realen Zeitfunktion eine komplexe Funktion hergestellt, welche zwei neue nützliche Eigenschaften besitzt — die Einhüllende und die Momentanfrequenz. Die praktische Anwendung der Einhüllenden wird demonstriert.

Introduction

The newly developed 2 ch. FFT analyzers, Types 2032 and 2034 incorporate discreetly a unique feature – the Hilbert Transform. Although the name Hilbert does not appear on the screen, this transform is manifested by the fact that all the normal real-valued time domain functions (Correlation, Impulse Response etc.) are in fact complex-valued functions in the 2032 and 2034. This is because the imaginary part of a

function is the Hilbert Transform of the real part. Hence, these time functions can be displayed similarly to the frequency domain functions in terms of their real part, imaginary part, magnitude, and phase, vs. time, with even "Nyquist" and "Nichols" plots being available. The magnitude describes the envelope of the signal, and since the magnitude is a positive quantity it can be displayed on a logarithmic amplitude scale, giving a large dynamic display range also in the time domain. This envelope function is similar to the Energy-Time Curve, or ETC, known from Time Delay Spectrometry. Also the phase representation is of interest, since it allows the detection of "instantaneous frequency", which is of importance for signals sweeping in frequency with time.

The main applications of complex time domain functions are found in propagation delay estimation (envelope of the Cross Correlation) and in the study of Impulse Responses ("Energy-Time").

While the Fourier Transform moves the independent variable of a signal from the time to the frequency domain or vice versa, the Hilbert Transform leaves the signal in the same domain. The Hilbert Transform of a time signal is another time signal and the Hilbert Transform of a frequency "signal" is another frequency signal.

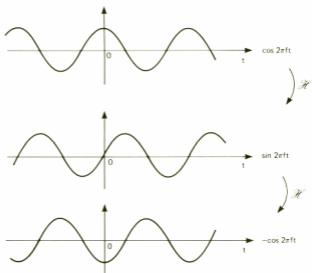


Fig. 1. Hilbert Transforms of a sinusoid

The simplest non-mathematical way of describing the Hilbert Transform of a time signal is to say that it gives all the frequency components of a signal a -90° phase shift, or in the time domain that it shifts each component by $1/4$ wavelength. This effect is similar to an integration of the signal. As an example, the Hilbert Transform of a sinusoid is shown in Fig.1. Using the letter \mathcal{H} to denote the Hilbert Transform it is seen that

$$\mathcal{H}(\cos 2\pi ft) = \sin 2\pi ft, \quad \mathcal{H}(\sin 2\pi ft) = -\cos 2\pi ft, \text{ etc.}$$

Notice that the shift is not a given time shift, but depends on the wavelength (or frequency) of the particular component.

Definition

The Hilbert Transform of a real-valued time signal, $a(t)$, is defined as

$$\mathcal{H}[a(t)] = \hat{a}(t) = \frac{1}{\pi} \int_{-\infty}^{\infty} a(\tau) \frac{1}{t-\tau} d\tau \quad (1)$$

However, before we can explore this equation without involving too much mathematics, we must provide ourselves with a few tools:

1. Symmetry properties of the Fourier Transform

$$a(t) \xrightarrow{\mathcal{F}} A(f) \xrightarrow{\mathcal{F}} a(-t) \xrightarrow{\mathcal{F}} A(-f) \xrightarrow{\mathcal{F}} a(t) \quad (2)$$

where \mathcal{F} means Fourier Transform.

From this it can easily be "seen" that

$a(t)$	$\xrightarrow{\mathcal{F}}$	$A(f) = R(f) + iX(f)$
real, and even		real, and even
real, and odd		imaginary, and odd
real		R even, X odd
imaginary		R odd, X even

TABLE 2

2. The convolution theorem

$$a(t) \star b(t) = \int_{-\infty}^{\infty} a(\tau) \cdot b(t-\tau) d\tau \quad (3)$$

$$a(t) \star b(t) \stackrel{\mathcal{F}}{\Leftrightarrow} A(f) \cdot B(f) \quad (4)$$

$$a(t) \cdot b(t) \stackrel{\mathcal{F}}{\Leftrightarrow} A(f) \star B(f) \quad (5)$$

where " \star " denotes "convolution". Equations 4 and 5 express the convolution theorem, i.e. the Fourier Transform of a convolution of two time signals is the product of the Fourier Transforms of the signals, and vice versa.

3. Sign function

$$\text{sgn } t = \begin{cases} +1 & t > 0 \\ -1 & t < 0 \end{cases}$$

has the following Fourier Transforms:

$$\mathcal{F}[\text{sgn } t] = \frac{1}{i\pi f} \quad (6)$$

and

$$\mathcal{F}\left[-\frac{1}{i\pi t}\right] = \text{sgn } f \quad (7)$$

Eq.6 is illustrated in Fig.2.

With these tools we can now rewrite Eq.1, recognising that the Hilbert Transform is a convolution (Eq.3):

$$\mathcal{H}[a(t)] = \hat{a}(t) = \frac{1}{\pi} a(t) \star \frac{1}{t} \quad (8)$$

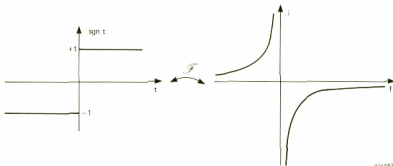


Fig. 2. Fourier Transform of $\text{sgn } t$

871243

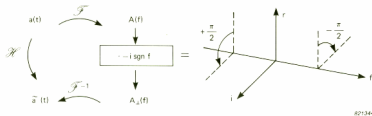


Fig. 3. The effect of the Hilbert Transform of a time signal as seen in the frequency domain

Using the Fourier Transform and Eq.7:

$$\mathcal{F} [\tilde{a}(t)] = A_{\perp}(f) = A(f) (-i \cdot \text{sgn } f) \quad (9)$$

The symbol " \perp " indicates that the phase of $A_{\perp}(f)$ has been changed by 90° , compared to that of $A(f)$.

Notice that Eq.9 states that in the frequency domain the Hilbert transform corresponds to a phase change of -90° ($-i$) for positive frequencies and $+90^\circ$ (i) for negative frequencies. This is illustrated in Fig.3.

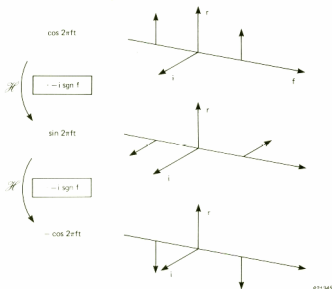


Fig. 4. Hilbert Transforms of a sinusoid as seen in the frequency domain

Fig.4 shows the Hilbert Transforms of Fig.1 as seen in the frequency domain.

Fig.3 also indicates an easy way of calculating the Hilbert Transform of a time signal: by Fourier transforming to the frequency domain, changing the phase of each of the frequency components by $\pm 90^\circ$, (depending on whether they are positive or negative frequency), and then inverse Fourier transforming back to the time domain.

The inverse Hilbert Transform (sometimes called the "Berthil" Transform) is defined in a manner similar to Eq.8 and Eq.9:

$$a(t) = \mathcal{F}^{-1} [\tilde{a}(t)] = -\frac{1}{\pi} \int_{-\infty}^{\infty} \tilde{a}(\tau) \frac{1}{t-\tau} d\tau \quad (10)$$

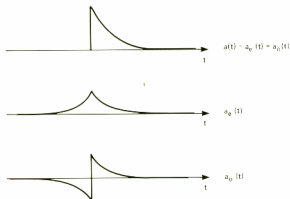
$$A(f) = A_{\perp}(f) \cdot (i \operatorname{sgn} f) \quad (11)$$

Therefore the inverse Hilbert Transform corresponds to a phase shift of 90° in an opposite direction to the Hilbert Transform itself.

Causal Signals

A signal, for example a time signal, is called **causal** if it equals zero for negative t :

$$a(t) = 0 \quad t < 0$$



621346

Fig. 5. A causal time signal shown as a sum of an even signal and an odd signal

As shown in Fig.5, such a signal can be written as a sum of an even signal $a_e(t)$ and an odd signal $a_o(t)$:

$$a(t) = a_e(t) + a_o(t)$$

Using the symmetry properties of the Fourier Transform we find

$$\mathcal{F} [a_e(t)] = R(f)$$

$$\mathcal{F} [a_o(t)] = iX(f)$$

and hence

$$\mathcal{F} [a(t)] = R(f) + iX(f)$$

For the causal signal $a(t)$, a_e and a_o are not independent of each other since

$$a_e(t) = a_o(t) \cdot \operatorname{sgn} t$$

hence, $R(f)$ and $X(f)$ must also depend on each other. Using the Fourier Transform and the convolution theorem we find

$$\mathcal{F} [a_e(t)] = \mathcal{F} [a_o(t) \cdot \operatorname{sgn} t]$$

$$\begin{aligned} R(f) &= iX(f) \star \frac{1}{i\pi f} \\ &= \mathcal{H} [X(f)] \end{aligned}$$

Hence for causal time signals, (e.g. the impulse response of a physically realizable system), we find that the real and imaginary parts of the system's frequency response are related by the Hilbert Transform.

For a Causal System:

Impulse Response $h(t) \quad (h(t) = 0 \quad t < 0)$

Frequency Response Function $H(f) = \mathcal{F} [h(t)]$
 $= R(f) + iX(f)$

where $R(f) = \mathcal{H} [X(f)] \quad (12)$

Notice that although this discussion has been concerned with causal time signals, the same relationships will apply to a causal (i.e. one sided) frequency signal.

Analytic Signals

Consider a time signal $a(t)$ and its Hilbert Transform $\hat{a}(t) = \mathcal{H}[a(t)]$. The analytic signal corresponding to $a(t)$ is defined as:

$$\begin{aligned}\check{a}(t) &= a(t) + i \hat{a}(t) \\ &= |\check{a}(t)| \cdot e^{i\theta(t)}\end{aligned}\quad (13)$$

where $|z(t)|$ is the magnitude or envelope:

$$|\check{a}(t)| = \sqrt{a^2(t) + \hat{a}^2(t)} \quad (14)$$

and $\theta(t)$ is the (instantaneous) phase:

$$\theta(t) = \tan^{-1} \frac{\hat{a}(t)}{a(t)} \quad (15)$$

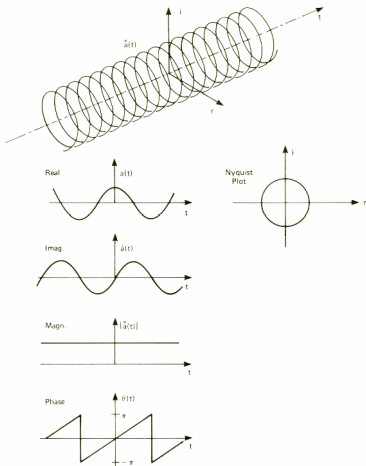
The rate of change of phase is the instantaneous frequency:

$$f_i(t) = \frac{1}{2\pi} \frac{d\theta(t)}{dt} \quad (16)$$

An example will help clarify this

$$\begin{aligned}a(t) &= \cos 2\pi f_o t \\ \hat{a}(t) &= \sin 2\pi f_o t \\ |\check{a}(t)| &= 1 \quad \text{i.e., a constant} \\ \theta(t) &= 2\pi f_o t \\ f_i(t) &= f_o\end{aligned}$$

In this case the analytic signal is a spiral revolving uniformly around the time axis as shown in Fig.6. The real part of the signal is a cosine, the imaginary part a sine, and the "Nyquist" plot (the signals projection on the real-imaginary plane, as seen along the time axis) is a circle. The magnitude is constant, and the phase is a linear function of time



821347

Fig. 6. The analytic signal of a cosine

increasing 2π per period, i.e., having a constant slope corresponding to the “instantaneous” (but constant) frequency f_0 .

Going back to Eq.13:

$$\tilde{\tilde{a}}(t) = a(t) + \hat{a}(t)$$

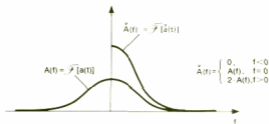


Fig. 7. The spectrum, $A(f)$, of a real time signal, $a(t)$, compared to the spectrum, $\tilde{A}(f)$, of the corresponding analytic signal, $\tilde{a}(t)$

we find using the Fourier Transform:

$$\begin{aligned} \tilde{A}(f) &= A(f) + i A_{\perp}(f) \\ &= A(f) + \operatorname{sgn} f \cdot A(f) \\ &= \begin{cases} 0 & f < 0 \\ A(f) & f = 0 \\ 2A(f) & f > 0 \end{cases} \end{aligned} \quad (17)$$

i.e. a one-sided spectrum is obtained, as shown in Fig.7. Hence, the analytic signal only includes the positive frequency components, i.e. the complex vectors rotating in the positive direction.

With the introduction of the analytic signal, we have finally abolished negative frequencies, but have introduced instead complex time signals. However, new useful properties are gained – the **Envelope** and **Instantaneous Frequency**.

A practical use of the envelope function is demonstrated in Fig. 8, where the Impulse Response of a system is shown in two different ways. The upper part shows the traditional presentation, i.e. the real part of the analytic signal on a linear amplitude scale. The lower part shows the envelope or magnitude of the analytic signal on a 40 dB logarithmic scale. It is clear that the lower presentation allows for a much easier determination of system delays (peak positions of the magnitude), and for a much more detailed study of the actual shape of the function.

APPENDIX

Causal Systems

For causal systems the Impulse Response $h(t)$ is causal, i.e. $h(t) = 0$ for $t < 0$

The Frequency Response is

$$\begin{aligned} H(f) &= \mathcal{F}[h(t)] \\ &= R(f) + iX(f) = A(f)e^{i\phi(f)} \end{aligned}$$

where $R(f) = \mathcal{R}[X(f)]$

Does a similar Hilbert transform relationship exist between the amplitude response $A(f)$ and the phase response, $\phi(f)$?

Yes – and no. For minimum phase systems there is a relationship.

Any Transfer Function $H(s)$ can be characterized by its poles and zeroes in the complex frequency plane – the s-plane.

$$H(s) = K \frac{(s-a_1)(s-a_2)\dots(s-a_n)}{(s-b_1)(s-b_2)\dots(s-b_m)}$$

where the a 's are zeroes and the b 's are poles.

Also such a Transfer Function can be written as a product of two parts:

$$H(s) = H(s)_{min} \cdot H(s)_{ap}$$

$H(s)_{min}$ is the so called minimum phase part, where all poles and zeroes are placed in the left hand half (real part < 0) of the s-plane, giving a minimum phase shift and hence the smallest delay between input and output for the given amplitude characteristic.

$H(s)_{ap}$ is an "all-pass" part, where the poles and zeroes are negative conjugates of each other i.e. of the form $\frac{s-a}{s+a^*}$.

The amplitude characteristic of this part is equal to one i.e. only the phase of $H(s)$ is influenced.

Hence $H(f)$ can be written as

$$\begin{aligned} H(f) &= A(f)_{min} \cdot A(f)_{ap} \cdot e^{i(\phi(f)_{min} + \phi(f)_{ap})} \\ &= A(f)_{min} \cdot e^{i(\phi(f)_{min} + \phi(f)_{ap})} \end{aligned}$$

It can be shown for the minimum phase part of the Frequency Response Function that:

$$\ln A(f)_{min} = \mathcal{H}[\phi(f)_{min}]$$

This relationship indicates, that for a given amplitude characteristic the Hilbert transform can be used to find the corresponding minimum phase characteristic. A proof of this relationship can be found in "The Fourier Integral and its Applications", p.204, McGraw-Hill, 1962, by A. Papoulis.

MICROPHONE SYSTEM FOR EXTREMELY LOW SOUND LEVELS *

by

Erling Frederiksen

ABSTRACT

This article shows how the thermal noise of microphone cartridges, caused by Brownian movements of the diaphragm, can be minimized, and how low inherent noise levels of preamplifiers are obtainable by optimisation and the use of modern components.

In an experimental system, third octave and A-weighted noise levels have been reduced by 16dB relative to conventional systems. This analysis has resulted in the development of a new low noise Condenser Microphone Type 4179 and a matching low noise Preamplifier Type 2660.

SOMMAIRE

Cet article montre comment le bruit thermique d'un microphone causé par le mouvement brownien du diaphragme peut être minimisé, et comment un faible niveau de bruit interne est obtenu pour le préamplificateur grâce à un choix et à une utilisation appropriés de composants modernes.

Un système expérimental a permis de réduire le niveau de bruit en tiers d'octave et pondéré A de 16dB par rapport aux systèmes classiques; et cette analyse a entraîné le développement d'un nouveau microphone à condensateur Type 4179 avec le Préamplificateur à faible bruit correspondant Type 2660.

ZUSAMMENFASSUNG

Der Artikel zeigt auf, wie das thermische Rauschen von Mikrofonkapseln, das durch Brown'sche Bewegungen der Mikrofonmembran verursacht wird, auf ein Minimum reduziert werden kann und wie sich niedriges Vorverstärker-Eigenrauschen durch optimale Auslegung und die Anwendung modernster Elektronik erreichen läßt.

Versuche haben gezeigt, daß sich A-bewertete und Terzband-Rauschpegel um 16dB gegenüber herkömmlichen Systemen reduzieren lassen. Diese Ergebnisse haben zur Entwicklung des neuen Kondensatormikrofons 4179 und des speziell auf diese Mikrofonkapsel abgestimmten Vorverstärkers 2660 geführt.

* Reproduced from 11th ICA Proceedings 1983.

Introduction

In some application fields, for example, hearing research, there is a need to measure very low sound pressure levels, in the order of -10 dB re. $20 \mu\text{Pa}$ in third octave bands or lower.

The lowest noise level microphone systems existing today, have typical inherent noise levels of 10 to 15 dB(A) or -5 to 5 dB in the third octaves between 20 Hz and 20 kHz. The noise spectrum of such a system is shown in Fig.1, curve A.

Since the lowest sound levels of interest cannot be measured by such systems directly, use must be made of advanced signal processing and time consuming procedures during which the experimental conditions may change. To overcome these difficulties, experiments have been carried out to reduce the inherent noise from the internal sources of the microphone systems. These noise sources are partly in the microphone cartridge and partly in the preamplifier. While the cartridge noise contributes to the spectrum A it has been eliminated in spectrum B in Fig.1, which shows the preamplifier noise only. For the measurement of spectrum B, the cartridge was substituted by an equivalent capacitor.

As can be seen, a significant noise reduction requires minimization of cartridge noise as well as preamplifier noise.

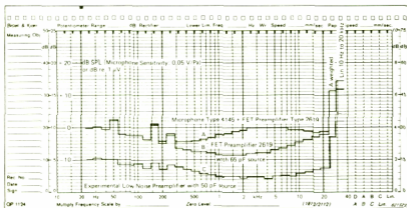


Fig. 1. Third octave analysis of Preamplifier output Noise Voltages

Experimental Low Noise Preamplifier

During the last 10 – 15 years the inherent noise of preamplifiers has been significantly reduced. This is mainly due to the Field Effect Transistor which has replaced the vacuum tube. The dominating noise sources of preamplifiers are described in the literature and shall not be discussed in this paper.

However, by appropriate component selection and careful optimization of the circuit, it has been possible to make experimental preamplifiers, having a 6 – 10 dB lower noise level than corresponding preamplifiers which are available today. With a source capacitance of 50 pF they have typically an A-weighted noise level of 0,7 μV and 1,2 μV for flat weighting from 20 Hz to 20 kHz; the noise spectrum of such an experimental preamplifier is shown in Fig.1, curve C.

The noise has been reduced to a level which corresponds to the noise of the input stage of modern measuring amplifiers. A low noise voltage amplifier has therefore been combined with the preamplifier to raise its output level by 20 dB, which thus eliminates the influence of the measuring amplifier noise. Extra filtration of the supply voltages has been necessary to minimize hum components in the noise.

Noise sources of Condenser Microphone Cartridges

Analysis of transducer characteristics are often simplified by use of equivalent electrical networks. This is also relevant in connection with analysis of inherent noise in microphone cartridges. A useful condenser microphone model is shown in Fig.2. In electrical as well as acoustical circuits Thermal Noise is produced by resistances or damping mechanisms. The noise pressure produced by an acoustical resistance is determined by the following formula:

$$\overline{p_n^2} = \int_{f_1}^{f_2} 4 \cdot K \cdot T \cdot R_a \cdot df$$

where

$\overline{p_n^2}$ = mean value of squared pressure

K = Boltzmann's constant

T = absolute temperature

R_a = acoustical resistance

f = frequency

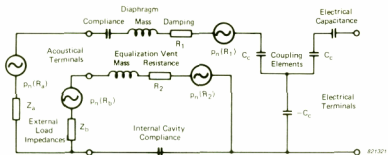


Fig. 2. Model of Condenser Microphone Cartridge

Inside condenser microphones there will normally be two such sources. One source belongs to the damping mechanism behind the diaphragm (R_1) and the other one to the resistance of the pressure equalisation vent (R_2).

The impedance loading the diaphragm on its outside (Z_a) has a real part (R_a) which also produces thermal noise. In principle there is a corresponding impedance (Z_b) and resistance (R_b) connected to the outside opening of the equalisation vent.

In the equivalent circuit the internal noise pressure generators can be treated as if they were connected to the respective acoustical input terminals. To determine the contribution of each noise generator to the overall cartridge noise, the spectrum of each generator should be multiplied by the transfer function between the respective acoustical input terminals and the electrical output terminals.

Since the typical resistance values of Type 4145 are known, their noise can be calculated. The two transfer functions from the acoustical inputs to the electrical output are also known; from the diaphragm terminals it is practically equal to the pressure response, as the outside load on the diaphragm, Z_a is small compared with the acoustical impedance of the diaphragm and its internal damping. The transfer function from the vent opening decreases by 20 dB/decade from the lower limiting frequency of the cartridge, 1.5 Hz to about 1000 Hz where it starts rolling off at a higher rate.

From the above it can be shown that the most significant noise source in Type 4145 is R_1 , the diaphragm damping. At frequencies below 30 Hz the vent resistance, R_2 is the most significant noise source.

Experimental Low Noise Microphone Cartridge

Since the most serious cartridge noise in Type 4145 and other existing microphones is produced by the diaphragm damping resistance, R_1 , experiments have been carried out to minimize this effect, resulting in the development of 1" cartridges having a resistance 40 times lower than that of Type 4145.

As it has not been practically possible to reduce the diaphragm mass and stiffness proportionally, the frequency response of the microphone cartridges changes significantly; a peak appears at the diaphragm resonance (8 kHz). However, an electrical network has been developed which compensates for the microphone response so that a flat response is obtained for cartridge and network up to 13 kHz within 1 dB, see Fig.3.

The sensitivity of the cartridges is increased by 6 dB compared to Type 4145; i.e. -20 dB re 1 V per Pa.

The sensitivity increase minimized the influence of the preamplifier noise correspondingly; also the compensation network which is combined with the preamplifier contributes to the noise reduction.

The damping resistance, R_1 , of the low noise microphone is typically $1,25 \cdot 10^6$ Ns/m^5 . It's noise pressure ($1,43 \cdot 10^{-7}$ $\text{Pa}/\sqrt{\text{Hz}}$ or -43 dB SPL for 1 Hz b.w.) is 16 dB lower than for R_1 of Type 4145. The output voltage noise spectrum is also 16 dB lower, as the transfer function of the

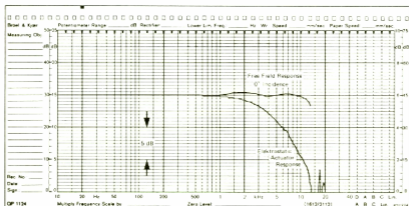


Fig. 3. Frequency Response of Experimental Low Noise Microphone System

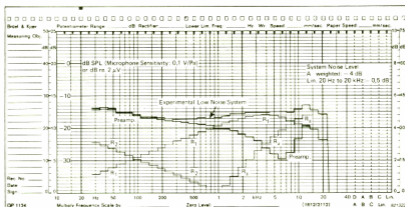


Fig. 4. Third octave analyses of the noise produced by the Experimental Low Noise Microphone System and of the individual elements

experimental cartridge with compensating network is the same as that of Type 4145, see the third octave spectrum in Fig.4.

Because of the significant cartridge noise reduction, the real part of the external load impedance, R_a has become a dominating noise source at higher frequencies, see spectrum in Fig.4. At 10 kHz R_a exceeds the internal diaphragm damping resistance, R_1 .

$$R_a = \frac{\rho \cdot f^2 \cdot \pi}{c} \cdot K_r^2 ;$$

$$R_a [10 \text{ kHz}] = 1,5 \cdot 10^6 \text{Ns/m}^5$$

ρ = density of the air;

f = frequency;

c = speed of sound;

K_r = ratio between random and pressure response.

The noise produced by the vent resistance, R_2 which is typically $6 \cdot 10^9 \text{Ns/m}^5$ is also shown in Fig.4. Due to the transfer response from the vent terminals, this noise will contribute to the output noise at low frequencies. However, it does not play any practical role, as the preamplifier noise is dominant in that frequency range.

The noise contribution of the external vent resistance, R_b , is very low and can be neglected.

The acoustical noise spectra have all been calculated, while the preamplifier noise spectrum which is also shown in the figure has been measured.

The noise source analysis explains clearly the measured total noise spectrum of the system.

The A-weighted levels of the preamplifier, the internal damping, R_1 , and the external load resistance, R_a are -10 dB, -7 dB and -11 dB respectively resulting in an overall level of -4 dB(A).

Conclusion

An experimental one inch microphone system with a flat frequency response up to 13 kHz has been developed; a system which is able to detect extremely low sound pressure levels — the inherent A-weighted noise of the system is -4 dB or about 15 dB lower than the noise of any corresponding systems.

References

- [1] BECKING, A.G.TH. & RADEMAKERS, A. "*Noise in Condenser Microphones*", *Acoustica* 4, 1954.
- [2] WHITTLE, L.S. & EVANS, D.H. "*A New Approach to the Measurement of very Low Acoustic Noise Levels*", *Journal of Sound and Vibration* (1972) 23 (1).
- [3] TARNOW, V. "*Thermal Noise in Microphones and Preamplifiers*", *Brüel & Kjær Technical Review* No. 3-1972.
- [4] MØLLER, P.K. "*Measurement of Background Noise in Sound Insulated Rooms*." *Proceedings of NAS-80*.

IMPROVED RMS AVERAGING WITH TRUE EXPONENTIAL RESPONSE USING THE B&K LEVEL RECORDER TYPE 2317

by

Leif Thomsen

ABSTRACT

The RMS averaging circuits in the new Portable Level Recorder Type 2317 have been designed, so that when using Fast or Slow, the averaging and indicator (display) characteristics are in accordance to the IEC 651 Standard for sound level meters. Examples of AC and DC recordings of various types of everyday noises are included in the article to illustrate this. Special averaging time of 15 ms has also been included in the recorder to measure reverberation times as low as 0,2s.

SOMMAIRE

Les circuits redresseurs du nouvel Enregistreur de niveau Type 2317 ont été conçus de façon à ce qu'avec les pondérations temporelles "Rapide" et "Lente" les caractéristiques du moyenneur et de l'appareil indicateur soient en accord avec la norme CEI 651 pour sonomètres. Des exemples d'enregistrements AC et DC de divers types de bruits courants illustrent cet article. Une constante de temps spéciale de 15 ms est incorporée dans l'appareil pour la mesure de temps de réverbération aussi courts que 0,2s.

ZUSAMMENFASSUNG

Durch die Schaltungen zur Effektivwertmittlung im neuen Tragbaren Pegelschreiber 2317, wird das Gerät bei Einstellung der Zeitbewertungen F(Schnell) oder S(Langsam), den Anforderungen für die Mittelungs- und Anzeigecharakteristik von Schallpegelmessern gemäß DIN IEC 651, gerecht. Der Artikel macht dies anhand von Beispielen für Gleich- und Wechselfspannungsaufzeichnungen verschiedener Geräuscharten deutlich. Der Pegelschreiber eignet sich durch die zusätzliche Mittelungszeit von 15 ms auch zur Messung von Nachhallzeiten die lediglich 0,2 s betragen.

Introduction

The development of the logarithmic RMS detector in hybrid form has made possible a revision in the design of the logarithmic Level Recorder, which for many years has been a very useful link in the measuring instrumentation chain for acoustics and vibrations.

Traditionally meter instruments have been used for measuring noise and vibration levels, and from the Level Recorders 2306 or 2307 hard copies showing the time history of level versus time have been available. The recordings of nearly steady levels have shown good agreement with the meter indication, but for large signal variations e.g. for measurements of impulse noise, the recorders have only partly been able to show the same response as that of the meter circuits. This is because of the different ways in which the averaging has been carried out. In the meter circuit RC weighting circuits have been used to average the signals, while in the recorders the averaging has taken place in the electromechanical writing system, controlled by a velocity servo giving equal response for rising or decreasing levels. The meter circuit on the other hand, has a quick response close to the final position, and thereafter a smooth exponential movement to the correct deflection of the pointer. For a sudden decrease in level the meter indication falls with a constant speed depending on the chosen time constant (see Appendix).

The correct response of the meter for various types of noise impulses are established in the IEC 651 Standard for Precision Sound Level Meters (formerly IEC 179). Here the acceptable errors from the theoretical response as a function of the pulse width are given.

For some years most of the B & K noise and vibration measuring instruments have contained a DC Log output, so that the recorder, if it is fast enough, should be able to follow in the linear DC mode and thus meet the requirements of the standards. However, the 2306 is not fast enough for the "Fast" response of short impulses. Therefore the new portable Level Recorder Type 2317 has improved DC response and is faster and easier to calibrate with other instruments. For the applications where AC output is the only, or the preferred possibility, the 2317 has been provided with AC Log recording facility using a special hybrid circuit LMS detector, which is in fact the very same as is used in one of the latest developed Sound Level Meters Type 2230. The requirements of the IEC 651 are thus met for "Slow" and "Fast" recordings.

The signal from the transducer (microphone, accelerometer etc.) is preamplified by a broadband linear AC preamplifier in the meter instru-

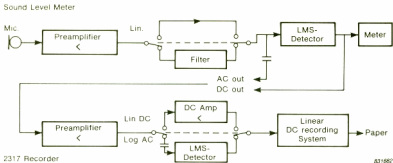


Fig. 1. General description of Measuring System

ment, Fig.1. The signal may then pass directly to the AC output, or through a filter or a frequency weighting circuit. After passing through the logarithmic RMS detector or any other sort of signal rectification and smoothing circuit a DC output may be obtained. If the AC output is used the recorder has to be in the AC Log mode. The dynamic range for the recording may be selected as 10, 25 or 50 dB. Using the DC output some additional possibilities are available e.g. other time constants (as provided by the meter instrument), other dynamic ranges, recording of L_{eq} and so on. For DC recordings the recorder is set in the LIN DC mode as the logarithm of the signal is taken in the meter circuit to give a linear dB scale.

As will be shown the two types of recording are identical and follow the meter fluctuations, if the meter and the writing system are both linear and fast enough to track the detector output within the accepted tolerances.

Examples of Recordings

Fig.2 shows four characteristic types of noise recordings obtained on a 2317, when the noise is measured using a Sound Level Meter Type 2230. The results on the left are obtained with the 2317 in AC Log mode with Fast RMS and 50 dB dynamic range. On the right the same results are obtained, but with DC recording. The paper speed for all recordings was 1 mm/s.

The two sets of recordings are seen to be quite identical. Fig.3 shows the noise from a type writing machine, recorded in different modes. The noise was recorded on tape and then played back and recorded on a

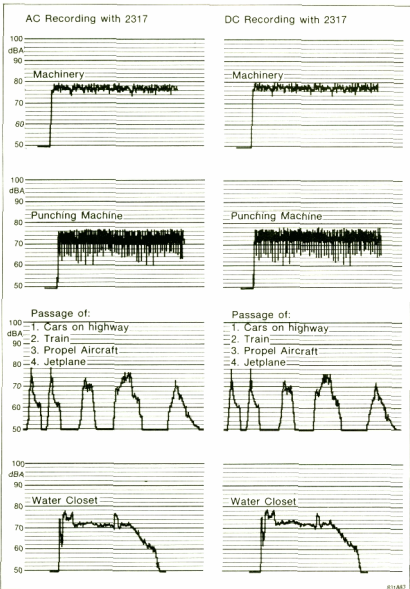


Fig. 2. Examples of Noise Recordings

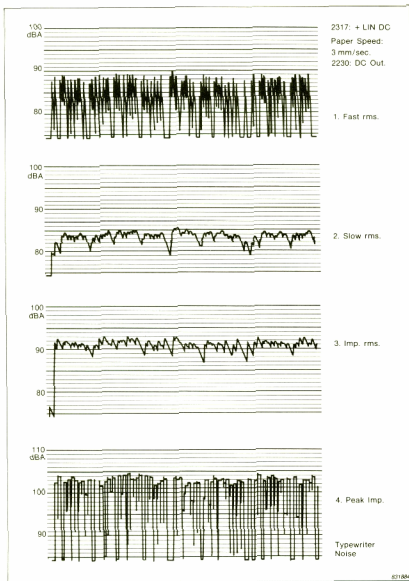


Fig. 3. Typewriter Noise recorded in different modes

2317/2230 combination (DC recording). The dynamic range was adjusted to 25 dB and the paper speed was set to 3 mm/s.

Long Time Noise Monitoring

When measurements are to be taken over a long period, the fluctuations make the reading rather uncertain on the chart recording. Here it is advantageous to use 60 s L_{eq} recordings from a 2225 Integrating Sound Level Meter. Fig.4 shows the same recordings of a music program using "Slow" averaging and 60 sec L_{eq} . The L_{eq} -curve shows more clearly the variations of sound level, although the breaks in the program are only seen in the "Slow" recording.

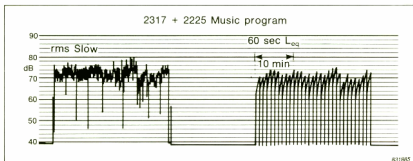


Fig. 4. Music program recorded in RMS Slow and 60 s L_{eq}

Measurements of Reverberation Time

In some applications the relatively slow response for decreasing levels is not convenient. For example when narrow peaks are recorded in a frequency response test or for reverberation measurements using an interrupted sound source and a sound level meter. In the last case the minimum reverberation time of 0,2 s requires a falling pen speed of 300 mm/s. A special averaging time of only 15 ms. has been provided to make that feasible. As the pen speed of the writing system is limited to 500 mm/s, the response is not truly exponential for increasing levels, which is however, irrelevant for this application.

APPENDIX

When a sound level meter is exposed to a step increase in input level, the exponentially weighted output from the meter circuit may be expressed as a function of time:

$$N = N_0 + 20 \cdot \log \sqrt{1 - \exp(-t/\tau)} \quad (\text{A.1})$$

where N is the indicated level in dB,

N_0 is the final level,

t is the time in s and

τ is the averaging time constant for the circuit.

It is assumed here that before the step the input is very small compared to the final level.

If the signal is suddenly removed, the output will fall off linearly:

$$N = N_{max} - (10 / \ln 10) \cdot (t - t_0) / \tau \quad (\text{A.2})$$

in which N_{max} is the level at the time t_0 when the signal is removed.

From the last expression it can be seen that the time constant may be determined from the rate of decrease. If the time for a 10dB decrease is called t_{10} and inserted in (A.2) the values:

$$N_{max} - N = 10 \text{ dB} \quad \text{and} \quad t - t_0 = t_{10} \text{ s,} \quad \text{and we get}$$

$$\tau = (10 / \ln 10) \cdot t_{10} = 0,4343 \cdot t_{10} \text{ s} \quad (\text{A.3})$$

The requirements in the IEC 651 for impulse sound meters are based upon the expression (A.1). As test signals, 2 kHz tonebursts with various duration t_s are used. The standard time constants are 1 s for "Slow" and 0,125 s for "Fast" response. The calculated results together with the accepted tolerances are shown in Fig.A1. The results of a test using a B & K Recorder 2317 in the AC Log mode are also shown here. The requirements are seen to be fully met.

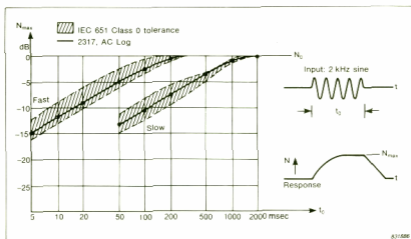


Fig. A1. IEC Tolerances for Fast and Slow

News from the Factory

Level Recorder Type 2317



The Portable Level Recorder Type 2317 is a fully portable unit designed for field and laboratory recording of DC and AC signal levels from $100\mu\text{V}$ RMS to 50V RMS, with frequencies up to 20kHz. It has DC and RMS response modes with choice of 10, 25 and 50dB logarithmic AC record ranges, plus two continuously adjustable linear DC record ranges. In the AC log mode the signal is fed through an RMS detector and an averaging circuit, giving a choice of four averaging times. The RMS detector conforms to IEC 651 Type 1 when used with the "Slow" (1 s) or "Fast" (125ms) time weightings. The "Vibr." setting gives a time constant of 2s mainly used for vibration measurements. The "Reverb." setting gives the pen a maximum fall speed of 300 mm/s, to measure reverberation times as low as 0,2s.

The writing system has two speeds and uses interchangeable fibre pens or sapphire styli. The recordings are made on 50mm wide pre-printed frequency-calibrated or lined paper as a function of frequency or time. Eight crystal controlled paper speeds are available. Start/stop and reverse of the paper drive can be remotely controlled. Additionally, the recorder has facilities for filter synchronization and external synchronization of the paper movement. The recorder can be powered from either built-in dry cells (standard), rechargeable Ni-Cd cells, from the mains via the plug-in Power Supply ZG 0199, or from an external DC supply.

Condenser Microphone Type 4179 and Preamplifier Type 2660



To facilitate measurements of very low sound pressure levels, Brüel & Kjær has developed a condenser microphone system consisting on one-inch diameter Condenser Microphone Type 4179 and Microphone Preamplifier Type 2660. This system is unprecedented in low-noise performance; the typical noise floor for the complete system is $-2,5$ dB(A), allowing measurements to be made down to levels of -5 to -15 dB in the third-octave bands between 20 Hz and 12,5 kHz. The frequency response is in accordance with IEC 651, Type 1 requirements, and the system is well-suited for laboratory hearing research, measurement and monitoring of very low background noise levels, and sound pressure and sound power level measurements of very-low-level sources.

Microphone Preamplifiers Types 2639 and 2645



For precision acoustic measurements with condenser microphones, two new microphone preamplifiers have been introduced to the Brüel & Kjær instrument range. The Preamplifiers have very low inherent noise, are robust, and are designed for use under a wide range of environmental conditions. Type 2639 accepts $1/2$ " microphones directly and 1 ", $1/4$ "

and 1/8" types via adaptors. It is intended for precision acoustic measurements in accordance with IEC, ISO and ANSI requirements. Type 2645 is similar in design and application to the 2639, but in addition includes a facility for insert voltage calibration of 1" and 1/2" condenser microphones in accordance with standards requirements throughout the world. Types 2639 and 2645 are available in two forms; delivered either in a mahogany case together with various accessories or alone in a plastic case.

Line-Drive Amplifier Type 2644 and Two Channel Power Supply Type 2813



The Brüel & Kjær Line Drive Amplifier is a miniature, unity-gain signal conditioning preamplifier, which can be mounted directly onto the top face of B & K accelerometers equipped with top connectors, or adjacent to accelerometers with side connectors.

Link-up with the new two-channel battery-operated power supply Type 2813 is via *single*, low-cost, coaxial cables which also carry the vibration signal from the accelerometer. This "Line Drive" system permits cable runs as long as 1 km to the measuring instrumentation without significant attenuation of the accelerometer/preamplifier sensitivity. A direct Line Drive input, which avoids the need for a separate power supply, is already provided in the new 2-Channel FFT Analyzers Types 2032 & 2034. The 2644 can be used integrally with an accelerometer in environments whose severity would normally restrict the use of other preamplifiers. It can endure mechanical shocks of up to 50 000 m/s² (~ 5000 g) and temperatures between -55° and 125°C.

Recorder Control Unit Type 7509



The Recorder Control Unit Type 7509 together with a front loaded Application Package, enables spectra, time functions and control settings from Brüel&Kjær Analyzers to be plotted by the X-Y Recorder Type 2308. The plots can be made to a preferred paper format and are in a fully annotated form which is suitable for direct inclusion in a report.

Two Application Packages are available: BZ 7075 for the Digital Frequency Analyzer Type 2131 and the Sound Intensity Analyzer Type 2134 (which is a part of the Sound Intensity Analysing System Type 3360) and BZ 7078 for the Narrow Band Spectrum Analyzer Type 2031 and the High Resolution Signal Analyzer Type 2033.

Four format modes are available for presentation of the measured data:

1. Dual half-size which plots two graphs of A5 size onto a sheet of A4 paper.
2. Single full-size which plots one graph onto a sheet of A4 paper.
3. Multiple full-size which plots a single group of control settings and several graphs onto the same sheet of A4 paper.
4. Preprinted format which plots one or more graphs onto preprinted A4 paper.

The total plotting time depends upon the chosen writing speed, the mode, the type of spectrum and the amount of relevant text. A single spectrum using the "Fast" writing speed may be plotted in 10s whilst a fully documented plot using "Slow" may take 2 minutes.

The X-Y Recorder Type 2308 may be fastened horizontally or vertically to the top of the Recorder Control Unit Type 7509 by means of the mounting brackets provided. Type 7509 is connected to the analyzer via

an IEC/IEEE interface cable and to the X-Y Recorder Type 2308 using the cables supplied, and the cabling is the same no matter what combination of analyzer and Application Package is employed.

Personal Noise Dose Meter Type 4434



The Brüel & Kjær Personal Noise Dose Meter Type 4434 is a handy, pocket-sized instrument for measuring the accumulated noise exposure of personnel in accordance with OSHA criteria. Designed to be worn by individuals without interfering with their working activities, it requires no special training to operate. The Dose Meter provides a continuous read-out of the total accumulated noise dose received by the wearer, expressed as a percentage of the maximum allowable daily noise exposure. The read-out is on a clear, easy-to-read display which may be concealed from the wearer by closing the front cover of the Meter.

In addition to noise dose, Type 4434 indicates when the noise level exceeds preset limits, above which exposure is considered to be acutely injurious to hearing and, in case of steady or continuous noise, is strictly prohibited by OSHA. Noise hazards as short as 100 μ s are detectable. This is of particular importance considering that the peak sound pressure level of transient and impulse types of noise is usually significantly higher than their loudness suggests. The Dose Meter also indicates when, the continuous noise has exceeded 115 dB(A), and/or 140 dB(A) peak for both continuous and impact noise.

Multiplexer Type 2514



A new Multiplexer, Type 2514, has been developed to provide multichannel facilities for Brüel & Kjær's permanent machine-vibration monitoring systems.

Designed specifically to complement the Type 2505 Vibration Monitor, the Type 2514 offers economical coverage of up to eight monitoring points. The Multiplexer continuously steps through the chosen monitoring channels, dwelling at each channel for a selectable period of between 1 second and 32 hours. Each channel has individual signal conditioning and sensitivity adjustment. The output from the multiplexer is fed to the vibration monitor, where the signal level is compared with preset limits to detect changes in the running condition of the machine. Danger levels detected by the vibration monitor are indicated by an alarm and by a light flashing at the relevant channel of the Multiplexer.

The Multiplexer and Monitor use modular circuit boards for easy maintenance and specification changes, and both comply with strict MIL standards to withstand harsh industrial environments. Other features of the 2514 include: A test cycle to check for malfunctions and incorrect settings; bypassing of individual channels; manual local- and remote-channel stepping; relay for external indication of a power failure; facility for external scan control, and an optional relay box for individual remote channel warnings.

The system can be further expanded by connecting a number of Multiplexers to one vibration monitor – up to a recommended maximum of 40 channels – and also be used for other AC signals such as sound.

PREVIOUSLY ISSUED NUMBERS OF BRÜEL & KJÆR TECHNICAL REVIEW

(Continued from cover page 2)

- 3-1977 Condenser Microphones used as Sound Sources.
- 2-1977 Automated Measurements of Reverberation Time using the Digital Frequency Analyzer Type 2131.
Measurement of Elastic Modulus and Loss Factor of PVC at High Frequencies.
- 1-1977 Digital Filters in Acoustic Analysis Systems.
An Objective Comparison of Analog and Digital Methods of Real Time Frequency Analysis.
- 4-1976 An Easy and Accurate Method of Sound Power Measurements.
Measurement of Sound Absorption of rooms using a Reference Sound Source.
- 3-1976 Registration of Voice Quality.
Acoustic Response Measurements and Standards for Motion-Picture Theatres.
- 2-1976 Free-Field Response of Sound Level Meters.
High Frequency Testing of Gramophone Cartridges using an Accelerometer.
- 1-1976 Do We Measure Damaging Noise Correctly?
- 4-1975 On the Measurement of Frequency Response Functions.
- 3-1975 On the Averaging Time of RMS Measurements (continuation).

SPECIAL TECHNICAL LITERATURE

As shown on the back cover page, Brüel & Kjær publish a variety of technical literature which can be obtained from your local B & K representative.

The following literature is presently available:

Mechanical Vibration and Shock Measurements

(English), 2nd edition

Acoustic Noise Measurements (English), 3rd edition

Architectural Acoustics (English)

Strain Measurements (English, German)

Frequency Analysis (English)

Electroacoustic Measurements (English, German, French, Spanish)

Catalogs (several languages)

Product Data Sheets (English, German, French, Russian)

Furthermore, back copies of the Technical Review can be supplied as shown in the list above. Older issues may be obtained provided they are still in stock.



BV 0015-11

Brüel & Kjær

DK-2850 NÆRUM, DENMARK · Telephone: + 45 2 80 05 00 · Telex: 37316 bruka dk